Landslides (2019) 16:633–645
DOI 10.1007/s10346-018-1107-9
Received: 4 March 2018
Accepted: 21 November 2018
Published online: 14 December 2018

Yasin Wahid Rabby · Yingkui Li

An integrated approach to map landslides in Chittagong Hilly Areas, Bangladesh, using Google Earth and field mapping

Abstract This paper presents a landslide inventory map for the Chittagong Hilly Areas of Bangladesh based on Google Earth and field mapping. We developed a set of criteria to identify landslides in Google Earth and introduced a method to assess the accuracy of mapped landslides when they are recorded as points rather than polygons in the field. In total, 230 landslides (mainly occurred between 2001 and 2016) were mapped in Google Earth. Field mapping identified 548 landslides and most of them occurred during Summer 2017. In total, the inventory includes 730 landslides for Chittagong Hilly Areas from 2001 to 2017. The field validation suggests that the accuracy of mapped landslides using Google Earth varies from 69 to 88%. Field work is preferred to map detailed landslides in or near urban areas, road networks, human settlements, and other accessible areas, while Google Earth has the advantage to map landslides in inaccessible areas. The combination of these two approaches provides a means to prepare the landslide inventory for an entire area.

Keywords Landslide inventory · Chittagong Hilly Areas · Google Earth · Field mapping · Criterion of detection · Accuracy assessment

Introduction

Landslide inventory mapping is an important step for landslide susceptibility, hazard, and risk assessment (Kanwal et al. 2016). Depending on the scale, a landslide can be mapped as a point or a polygon, and various techniques have been used for landslide inventory mapping (Guzzetti et al. 2012). Traditional methods include the interpretation of aerial photographs, satellite imagery, and field mapping. These methods are commonly used to generate the landslide inventory for a large area (Alkevi and Ercanoglu 2011). Data obtained from the literature, newspaper, journals, technical reports, governmental archives, and expert interviews are also used to prepare landslide inventories for small areas (Glade 1998). In recent years, landslides have also been mapped using high-resolution digital elevation models (DEM), light detection and ranging (LiDAR), and synthetic aperture radar (SAR) data (Guzzetti et al. 2012).

Bangladesh is a primarily low-lying floodplain country in South Asia. Mountainous terrain in the north and southeast covers only 18% of the country. Landslides are common in the hilly regions, especially the Chittagong Hilly Areas (CHA) (Fig. 1) in southeastern Bangladesh (Banglapedia 2015). Most landslides occur during the monsoon season in the CHA due to extreme rainfall (> 40 mm/day) within a short period (2–7 days) (Khan et al. 2012). High cloud cover during this season prevents the identification of landslides from high- (0.5–5 m) and medium- (15–30 m) horizontal resolution multi-spectral images, such as Landsat imagery. Regional or local high-resolution aerial photographs and imagery are either not available or not accessible for free in this area. In addition, vegetation regrows quickly after a landslide event in this subtropical area, presenting a challenge to identify the landslide using satellite images or aerial photographs a few months after the event (Samodra et al. 2015).

Most landslide inventory studies have focused on the major cities in CHA (Ahmed 2015 and CDMP-II 2012). For example, Ahmed and Dewan (2017) and Ahmed (2015) compiled landslide inventories for Chittagong Metropolitan Area (CMA) and Cox's Bazar municipality and developed different techniques in landslide mapping. In contrast, few studies have been conducted outside of these cities. We used the visual interpretation of multi-temporal imagery in Google Earth and extensive fieldwork to map old and recent landslides in CHA. The landslides identified using these two methods are combined to produce a landslide inventory map. High-resolution multi-temporal Google Earth imagery allows for identifying landslides in remote areas where field mapping is not possible. Several studies have used Google Earth for landslide mapping (Sato and Harp 2009; Fisher et al. 2012; Vakhshoori and Zare 2016). Sato and Harp (2009) developed five criteria for detecting rock falls and rock slides caused by an earthquake event from a single Google Earth image. Based on these studies, we applied four criteria for detecting landslides (mainly triggered by rainfall) in Google Earth in CHA. We also introduced an accuracy assessment method for Google Earth-based landslide mapping.

Study area

The Chittagong Hilly Area (Fig. 1) (20,957 km^2) is located in the southeast of Bangladesh (20.46–23.40° N and 91.27–92.18° E) and includes five districts: Bandarban, Rangamati, Khagrachari, Chittagong, and Cox's Bazar. CHA has a tropical monsoon climate with the annual rainfall ranging from 2540 mm in north and east to 2794 to 3777 mm in south and west. This area has three distinct seasons: The dry and cool season from November to March, the hot or pre-monsoon season from April to May, and the monsoon or rainy season from June to October (Banglapedia 2015). About 80% of the landslides occur between May and September when the average monthly rainfall is > 480 mm (CDMP-II 2012).

The hilly area can be divided into the low (< 300 m) and high hill ranges (> 300 m) (Banglapedia 2015). The low hill ranges are under Dupi Tila and Dihing formation, whereas the high hill ranges under Surma and Tipam formation (Fig. 2) (Brammer 2012). Most of the western areas have slopes < 5°, while the areas in the east have slopes > 30° (Fig. 2).

Data source

We used Google Earth imagery and existing landslide database to generate the inventory map. Google Earth contains available Landsat imagery (30 m or 15 m pan-sharpened), orthophotos (0.5–2 m), and high-resolution commercial satellite imagery (SPOT, FORMOSAT-2:

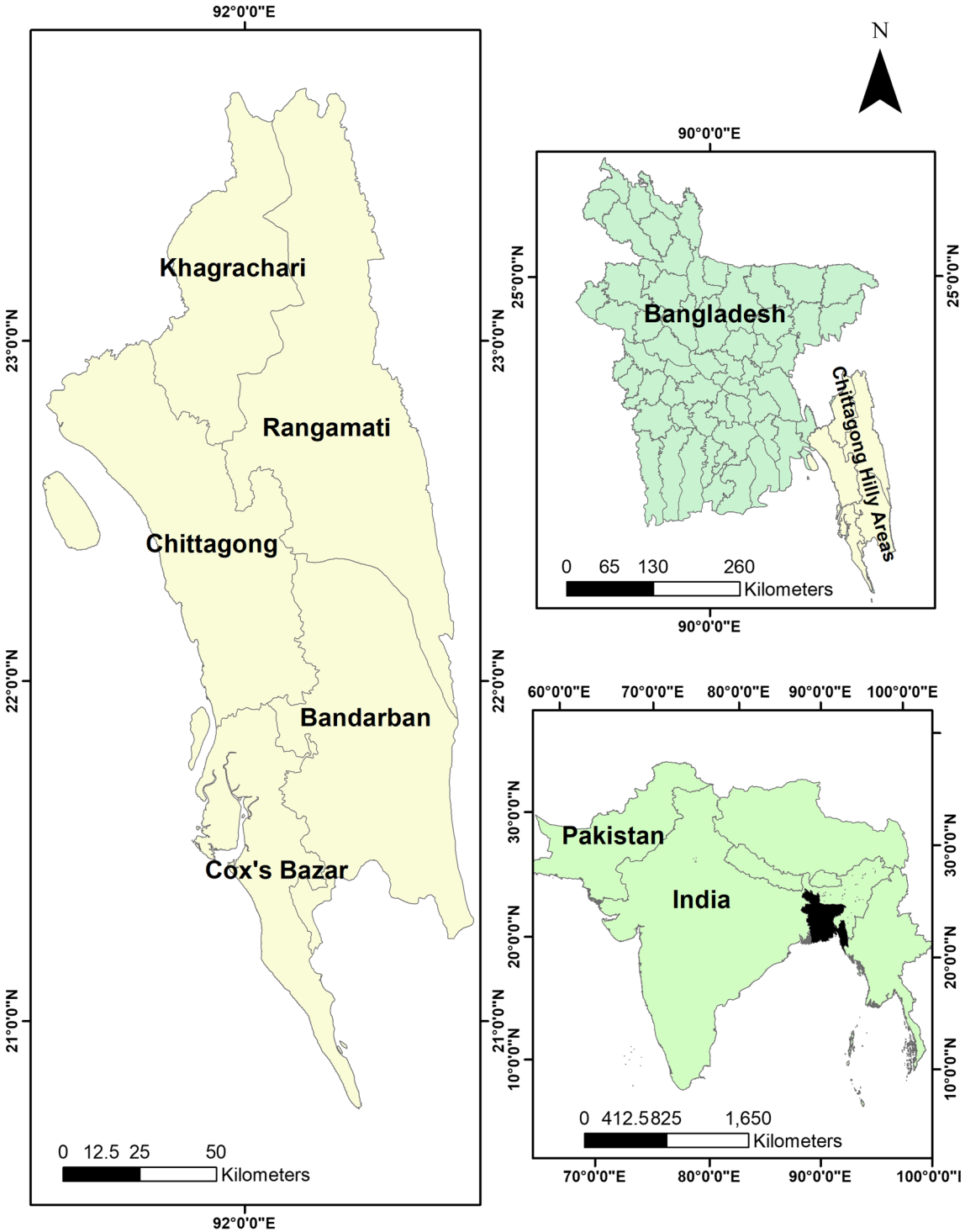

Fig. 1 Geographical position of Chittagong Hilly Areas

0.5–8 m; World View-1 and World View-2, 0.5–2.5 m) (Fisher et al. 2012; Crosby 2012). Google Earth shows different types of the imagery based on the scale and lists the provider of the imagery on screen. For example, Landsat imagery are provided by Terra Metrics, Inc., and World View images are provided by Digital Globe. For our study area, the high-resolution images are provided by Digital Globe. The terrain in Google Earth is represented using Shuttle Radar Topographic Mission (SRTM) (30- or 90-m resolution) or NOAA Global Land One-km Base Elevation Project (GLOBE) digital elevation models (DEMs) (Wang et al. 2017). These DEMs are also used to derive the slope and terrain profile in the add path tool (Fisher et al. 2012; Wang et al. 2017).

Bangladesh does not have an official database for landslides. The Department of Disaster Management (DDM) of the Ministry of Disaster and Relief of Bangladesh records landslides without

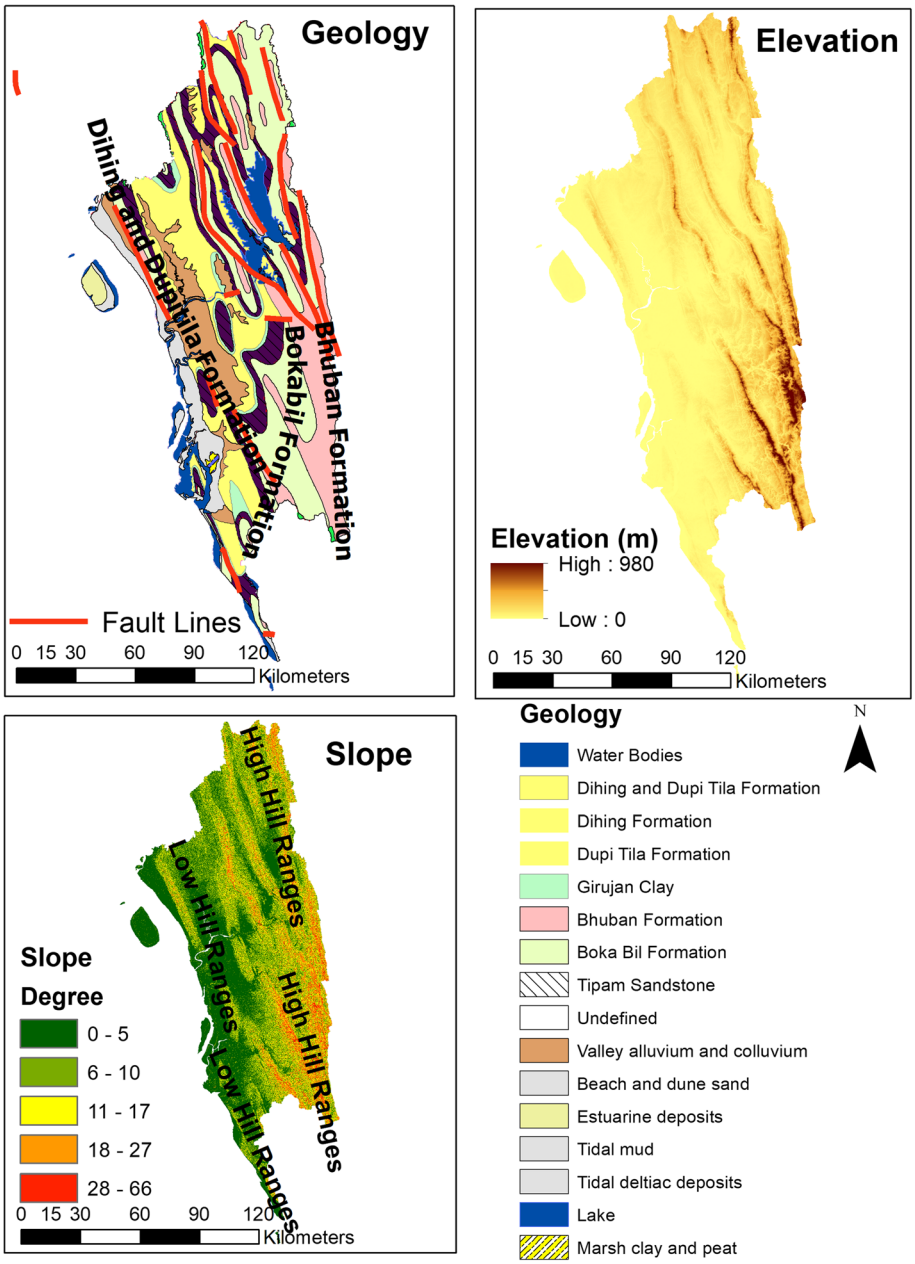

Fig. 2 Geological, slope, and elevation maps of Chittagong Hilly Areas

detailed locations. Most recorded landslides have the locational information only to the low-level administrative division, such as name of the village. This record is not updated regularly and not available online. The Comprehensive Disaster Management Programme of the Ministry of Disaster and Relief of Bangladesh provides a detailed landslide inventory for Cox's Bazar and Teknaf municipality areas (CDMP-II 2012). Rahman et al. (2016) provided landslide inventory for the Chittagong Metropolitan Area (CMA). These inventories contain GPS coordinates, extent, fatalities, and estimated economic loss caused by the landslides. Newspaper reports on landslides can be another data source as they provide the description of where, when, and why landslides occurred, how many people died, and estimated economic loss. However, these reports lack detailed locations and dimensions of the landslides.

Methods

The methodology includes four steps: (1) visual interpretation of Google Earth imagery, (2) field data collection and mapping, (3) field validation and accuracy assessment, and (4) final map production.

Visual interpretation of Google Earth imagery

Based on the availability of Google Earth imagery, landslides were mapped from January 2001 to March 2017. To keep track of mapping and prevent visual interpretation of an area more than once, the whole region was divided into 4911 rectangles (3.3 km long and 1.3 km wide) (Fig. 3f). These rectangles were created using the Fishnet tool in ArcGIS and then converted to a KML file. We

started the mapping from the upper-left rectangle (near the Feni river where the Chittagong District starts) and checked the images from left to right in each rectangle. The landslides were identified in Google Earth based on four criteria: change of vegetation in historical images (vegetation was absent and presence of bare land in one image but presence of vegetation in previous images), morphological change in historical images, the slope and elevation of suspected areas for landslides, and the presence of debris or deposits at the toe of suspected areas.

The Google Earth images from 2001 to 2017 were examined to detect changes in vegetation and morphology (Fig. 3a and b). Landslides can remove or destroy the vegetation of an area to

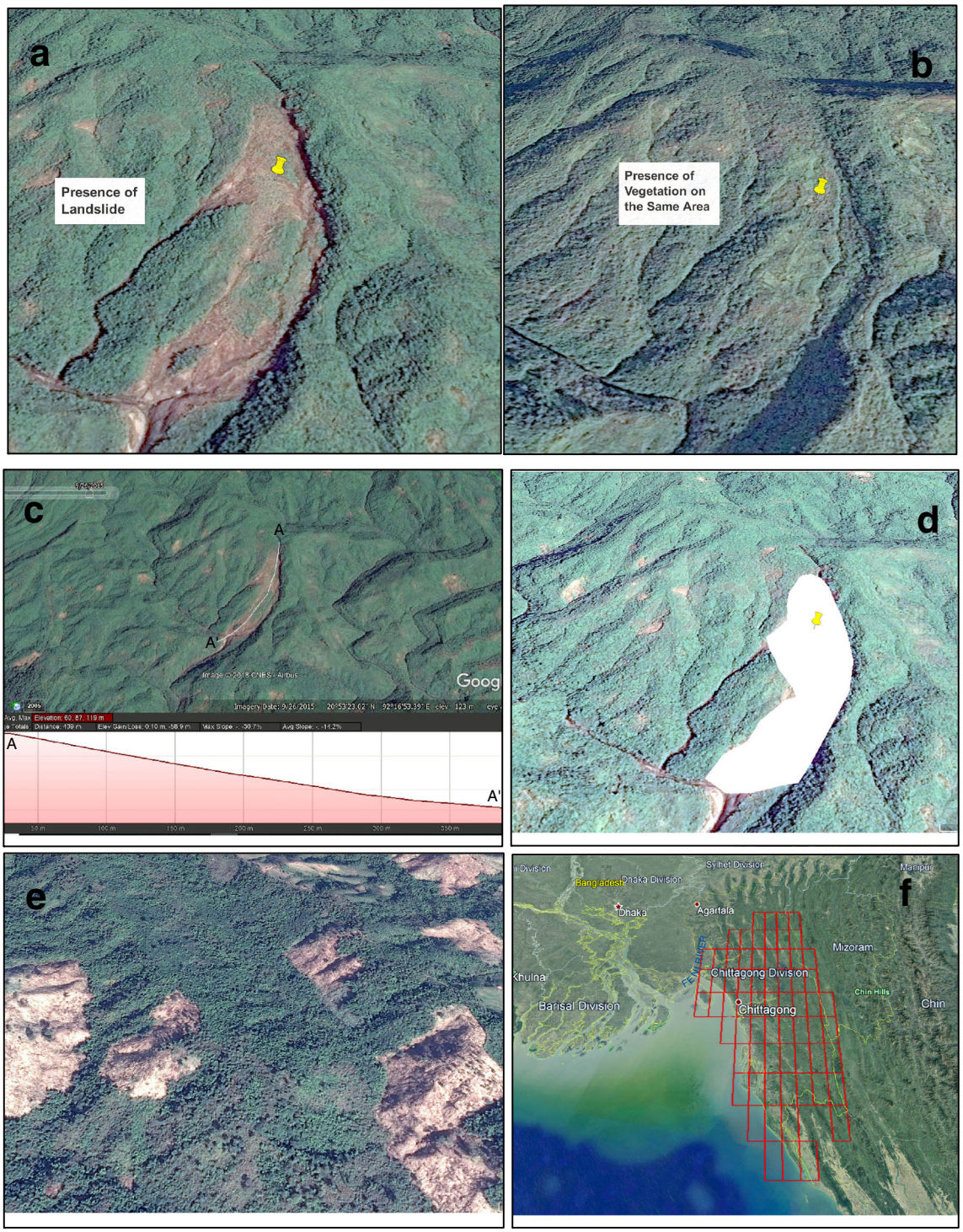

Fig. 3 Landslide detection in Google Earth. **a**, **b** Change detection and identification in Google Earth. **c** Landslide identification through elevation profile in Google Earth. **d** Polygon drawn around the scarp and run out of landslide. **e** Presence of clear cut. f Fishnet

expose bare land. However, open fields, vegetation removal due to flooding, and harvested paddy fields can also appear as bare land in Google Earth. The slope and elevation were measured to separate these different possibilities because landslides usually do not occur on a gentle slope (Duric et al. 2017). The changes in slope and elevation from the top to the bottom of a suspected area or the topsoil scarp indicate that landslide has removed topsoil and vegetation. The Add Path tool in Google Earth was used to check the slope of the bare land. This tool generates the topographic profile along the path (line or polygon) (Bailey et al. 2012). We drew a central line through each bare land (Fig. 3c) to examine the slope and elevation change along the profile. When a landslide occurs, topsoil and soil are generally deposited at the toe. This deposit was considered as an indication of landslides. Presence of mottling in the image help to detect debris or deposits of landslides. Due to morphological change, landslides have dark brown color or brighter contrast compared to the pale surrounding area. We went through Google Earth images using a constant eye altitude of 300 m to track all these changes and identify landslides. Zoom in and out tools were used when the eye altitude was not enough to detect these changes.

In our study, the change in vegetation was the first indicator of landslides. Next, morphological change and the presence of debris at the toe were checked. The presence of debris depends on the quality (resolution) of the image: we did not find this evidence in all mapped landslides because high-resolution images are not available in all areas. Thus, our primary criteria for the landslide identification are identifying changes in vegetation and morphology through the historical images, and measuring both slope and elevation along the profile. The presence of debris is optional, although it increases the mapping confidence when available. We also determined the type of movement (falls, topples, slides, spreads, and flows) according to Cruden and Varnes (1996) and drew polygons (Fig. 3d) around the scarp and run out (if identifiable). These polygons were saved to KML files in Google Earth. The identification of the landslide type depends on the quality of image. It is difficult to identify the material type through visual interpretation; thus, we did not include this information in the landslide classification scheme of Cruden and Varnes (1996).

Jhum (traditional shifting cultivation) is a common practice of plantation in CHA. It is a type of rotational farming: one slope of the land is cleared by controlled burning for cultivation, before it is left to regenerate after few years (Masum et al. 2011). Rotational cultivation is the principal driving force for vegetation removal in hilly forest areas of tropical Asia (Fox et al. 2000). In our method, removal of vegetation is considered as one of the primary indicators of landslides. Thus, in CHA where jhum cultivation is practiced, there is a high chance that these areas can be misinterpreted as landslides (Fig. 3e), as the land is left barren after the harvesting of crops and remains fellow for next seasons. The availability of historical images in Google Earth helps differentiate areas under jhum cultivation from landslides. We explored the pre and post images of the bare land to check the presence of jhum crops in that area. In addition, farmers usually select a rectangular or square slope area for slash-burning and crop cultivation. After harvesting the crops, the barren area is usually a rectangular or square shape. In contrast, a landslide is a natural process and its boundary (scarp or run out) is usually irregular.

Field data collection and mapping

Landslide records from local newspaper and existing literature, including published and unpublished articles, thesis, and reports, government documents and archives, and available inventory maps, were used for the field mapping (Table 1). Experts, officials of Disaster Management Department of People's Republic of Bangladesh, city planners, and local political leaders were interviewed to determine which areas are vulnerable to landslides, why landslides occur in addition to heavy rainfall, and whether there is any change in the pattern of landslides. We collected newspaper reports on landslides from 1980 to July 2017 at the library of the University of Dhaka. The data collection was mainly based on three Bengali newspapers (The Daily Ittefaq, The Daily Inqilab, and The Daily Prothom Alo) and two English newspapers (The Daily Observer and The Daily Star). We hired four data collectors because digital copies of these newspapers were not available. Data collectors went through a 3-h training program on how to collect data from newspapers before starting the data collection. The data collectors collected the date, time, and locations of landslides, number of death and injured, damage to infrastructures, and types and causes of landslides. Some reports provided the name of the vulnerable areas and the areas where people are living at the base of excavated hills. These reports helped identify target areas for field investigation and mapping. Local offices of Roads and Highways Department of the People's Republic of Bangladesh provided the locations of landslides that occurred along the roads during June 2017 under their jurisdictions. Most landslides we collected occurred near roads and human settlements in both rural and urban areas.

We adopted participatory field mapping proposed by Samodra et al. (2015) and used the collected landslides from newspapers and existing literature for field checking and mapping. Most collected data provide the general areas where landslides occur or are vulnerable to landslides without detailed locations (latitudes and longitudes). We asked local people, political leaders, governmental officials, and aid agencies to help find these locations. The field mapping was carried out from July to August 2017. A group consisted of five members (one group leader and four field assistants) were involved in the field mapping. All field assistants are college students with the training in geomorphology theory and field work. They are confident to identify landslides in the field. The group leader also conducted a final verification to make sure all data are recorded correctly. A GPS receiver (Gramin Trex 20x) with an accuracy of 3–10 m was used to collect the latitude and longitude information of each landslide (Fig. 4a, b, c, d). Chain and tape were used to measure the length and width of the landslide. In some cases, the GPS coordinates were measured 3–10 m away from the landslides due to the dangerous field conditions. We measured the distance between the GPS location and the landslide using chain or tape. We checked all collected locations in Google Earth to verify whether they are on the right locations. We did not measure the extent of the landslide in the field due to the lack of topographic maps. Instead, we measured the length and width of each landslide.

A form was used to record time and date (if available), landslide characteristics (if recognizable), land use and land cover type of the area, and visually identifiable causes and categorical damage assessment. We first visited each targeted area and then checked with the local people (Fig. 4e, f,) on whether landslides occurred or

Table 1 List of main landslide information sources

Source of information	Information collected
Local newspaper	Date, time, and locations of landslides
Rahman et al. (2016)	57 landslide locations of CMA
CDMP-II (2012)	77 landslide locations of Cox's Bazar and Teknaf municipalities
Records of Department of Disaster Management of People's Republic of Bangladesh	Name of the locations of landslide that caused casualties
Roads and Highways Department	Locations of landslides that caused road damages

not in the area. In some cases, the database from the Department of Disaster showed that landslides occurred on completely flat lands, and local people also failed to remember any landslide events there—this indicates the possibility of errors in the government database. Landslides that occurred in June 2017 were easily identifiable in the field. All recent landslides occurred within the landslide prone areas identified from newspaper reports. Most landslides we mapped in the field were new landslides, due to the high number of recent occurrences. Motorbikes and three wheelers were used to make sure that the survey was conducted as quickly as possible. On average, we mapped around 25 landslides per day. We took photographs of each landslide and its surrounding area to help verify the landslide characteristics that we identified during the field investigation.

Validation and accuracy assessment

Several methods are available for the validation and accuracy assessments of landslide mapping. Carrara et al. (1992) introduced a method based on the polygon overlay for the landslide validation and accuracy assessment. This method, however, does not consider the uncertainty, errors, and subjectivities of mapped landslide boundaries. Galli et al. (2008) suggested to use a 100-m buffer around landslide polygons as a threshold to account for the uncertainties and errors in landslide mapping. It treats the landslides (polygons) mapped from satellite imagery and the landslides mapped in the field the same if they are within 100 m of each other. We adopted this 100-m distance threshold in our study. However, we mainly recorded the landslides as points in the field, whereas delineated landslides were recorded as polygons in Google Earth. It is also not possible to check all Google Earth-identified landslides in the field. We chose three sites (Fig. 5) for the validation and accuracy assessment. We conducted the field mapping in a test site at Bandarban and compared with landslides that we identified in Google Earth. The next site was the Chittagong Metropolitan Area (CMA). We did not conduct field mapping in the CMA but Rahman et al. (2016) provided 57 landslide locations. The third site was Cox's Bazar municipality where CDMP-II (2012) provided 77 landslide locations. Some landslides provided by these two reports were not used in our study because they occurred in the 1990s—the oldest landslide that we detected in Google Earth occurred in 2003. We used the proximity of the landslides from two inventories (landslide points in field mapping and landslide polygons in Google Earth) to assess the accuracy. Specifically, if a landslide mapped in Google Earth is < 100-m difference compared with the landslide point in the field, we treat them as matched landslides. The Near tool in ArcGIS was used to determine the nearest distance between the Google Earth-mapped landslides and their closest landslide points recorded in the field (ESRI 2014). Based on the threshold distance of 100 m, the overall accuracy can be defined as:

$$X = \frac{a}{b}$$

where X is the overall accuracy, (a) is the number of landslides mapped in Google Earth that are within 100-m distance from landslide points recorded in the field, and (b) is the total number of landslide points recorded in the field. In addition, we also examined the commission and omission errors. The commission error refers to the percentage of misidentified landslides in Google Earth (> 100 m from the landslide recorded in the field). The omission error refers to the percentage of landslides that were recorded in the field, but not identified in Google Earth.

Final inventory map production

The final inventory map represents the integrated landslide maps from Google Earth, field mapping, and landslide locations provided by Rahman et al. (2016) and CDMP-II (2012). Same landslides identified in both Google Earth and field mapping were removed using the Select by Location tool in ArcGIS to avoid duplication. The feature type of the landslides is point in the final inventory map.

Results

Visual interpretation of Google earth imagery identified 230 landslides that occurred between 2003 and 2016 (Fig. 6a). In the field, we recorded 414 landslides. We also included 57 landslides in CMA provided by Rahman et al. (2016) and 77 landslides in Cox's Bazar and Teknaf municipalities provided by CDMP-II (2012). In total, we collected 548 landslides based on field mapping (Fig. 6b). The field mapping covered accessible areas where landslides were reported, and the field-recorded landslides mainly occurred in June 2017 (356 out of 548). Among these recent landslides, 305 of them occurred in the landslide prone areas that were mentioned in newspaper reports, and 51 occurred in new areas. In Bandarban, 101 landslides were identified—of these, 25 occurred before June 2017 with the oldest dated back to 1993. In Rangamati, all field-mapped landslides occurred during June 2017. Among 82 landslides in Khagrachari, only 12 of them occurred before 2017. Out of 137 field-mapped landslides in Chittagong, 74 landslides occurred before 2017. Table 2 shows the

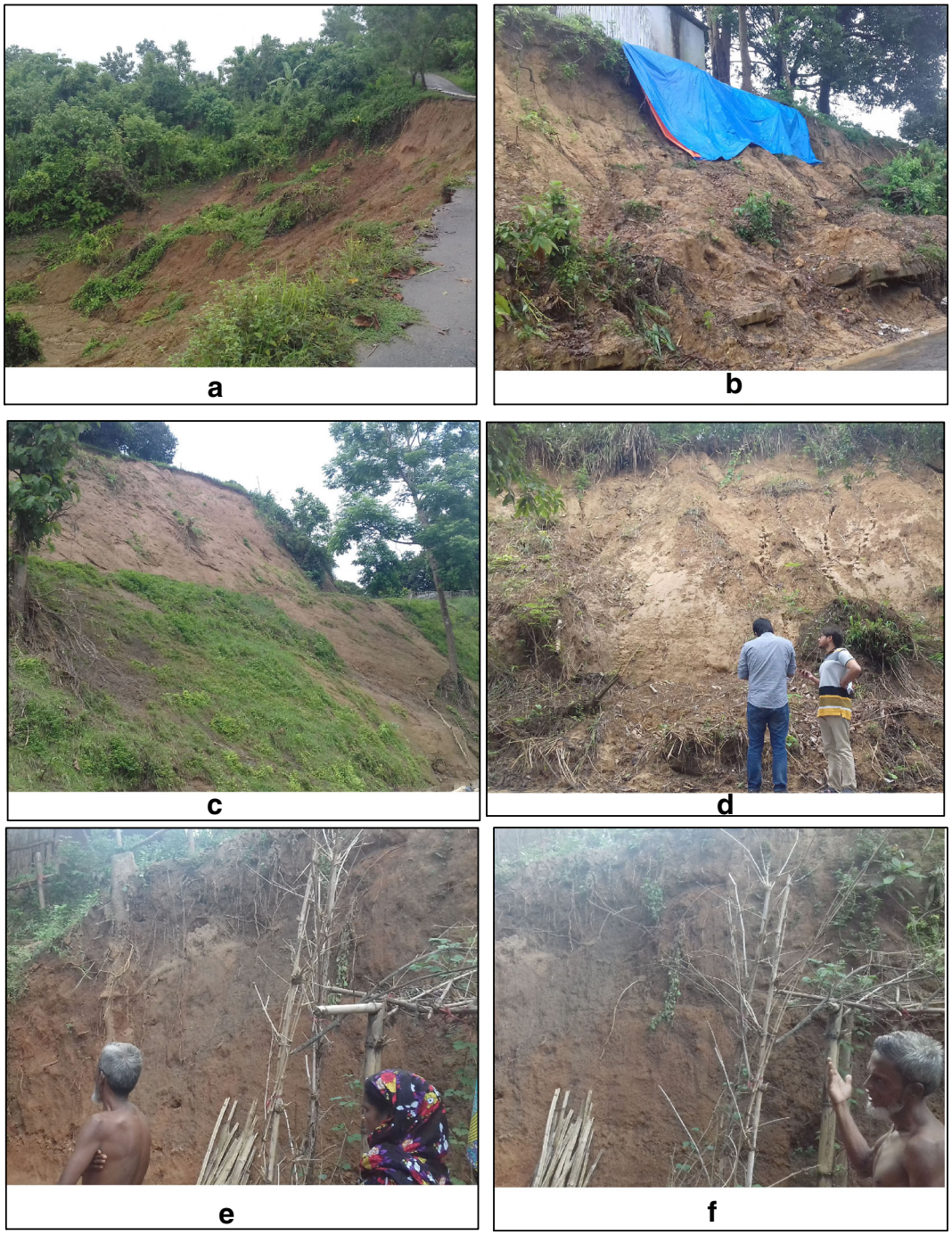

Fig. 4 Field mapping. **a**, **b** Field mapping with the assistance of local people. **c**–**f** Identification of landslides and GPS coordinate collection

distribution of the landslides identified in Google Earth and field mapping in the CHA. The mean elevation of landslides identified in Google Earth is 127.3 m (standard deviation (SD) = 121.0 m), the maximum elevation is 652.0 m, and 85% of the landslides are less than 200.0 m (Fig. 7a). For landslides identified in the field mapping, the mean elevation is 72.0 m (SD = 121.0 m), the maximum elevation is 483.0 m, and about 82% of the landslides are less than 100.0 m (Fig. 7a). Identifying the type of landslide in Google Earth is dependent upon the quality of the imagery and the skill of the interpreter. Among 230 landslides mapped in Google Earth, 62 were undefined due to the difficulty in determining their types. Slide is the dominant type of landslide, with flow and fall being two other major types identified in Google Earth (Fig. 7b). Among 15 unrecognized landslides, 12 are from Cox's Bazar district because we did not carry out the fieldwork there and landslide locations were provided by CDMP-II (2012). In field mapping, flow is the dominant type,

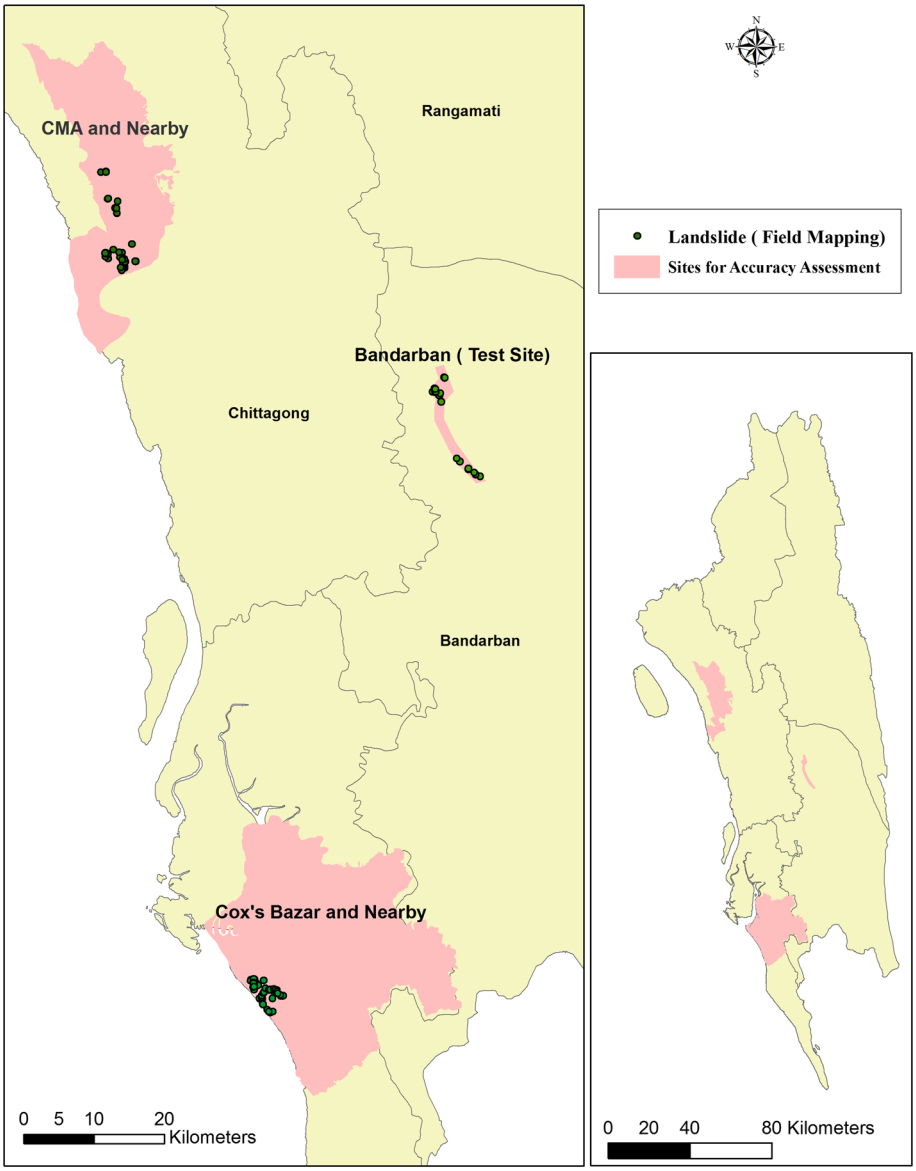

Fig. 5 Location of study sites for map validation and accuracy assessment

accounting for 40% of the total landslides (Fig. 7b). Slide is the second dominant type. There are also 28 complex landslides, which are combination of two or more types of landslides. Most field mapped landslides are shallow landslides (depth less than 10 m) with only 20 (out of 548) deep landslides, which are large slope failures with depths of > 10 m. Figure 8 (panels a–d) shows the distribution of slide, flow, fall, topple, and complex types of landslides over the study area. As mentioned before, slide and flow are the two dominant types of landslides and they have similar type of distribution (Fig. 8a, b). It seems that the type of geology, land use land cover, or presence or absence of fault lines do not affect the type of landslides in CHA.

The final landslide inventory (Fig. 6c) includes the locations of 730 landslides, as well as their types, areas (Fig. 8a, b, c, d), and time of occurrence. About 48.8% (356 out of 730) of the landslides in the inventory are recent landslides. This dataset is the largest landslide inventory of the CHA (Fig. 6c). The mapped landslides are clustered in some specific areas (Fig. 6a, b, c). The clusters are associated with the natural factors that influence landslides and the areas covered during field mapping. For example, landslides are clustered near the fault lines and in areas where the slope gradient is between 10 and 30°. Our field mapping was mainly in urban areas and along roads.

The validation and accuracy assessments were conducted in three sites: test site in Bandarban, CMA, and Cox's Bazar municipality. In our test site, we identified 25 landslides during field mapping and 22 landslides in Google Earth. All these landslides are < 100 m buffer distance from the landslides identified in the field mapping (8 have 0 distance) (Table 3). Therefore, the overall accuracy is 88% using the 100-m threshold buffer. The commission error is 0%, indicating that all landslides identified in Google Earth are actual landslides (Table 4). The omission error is 12%, indicating that 12% of

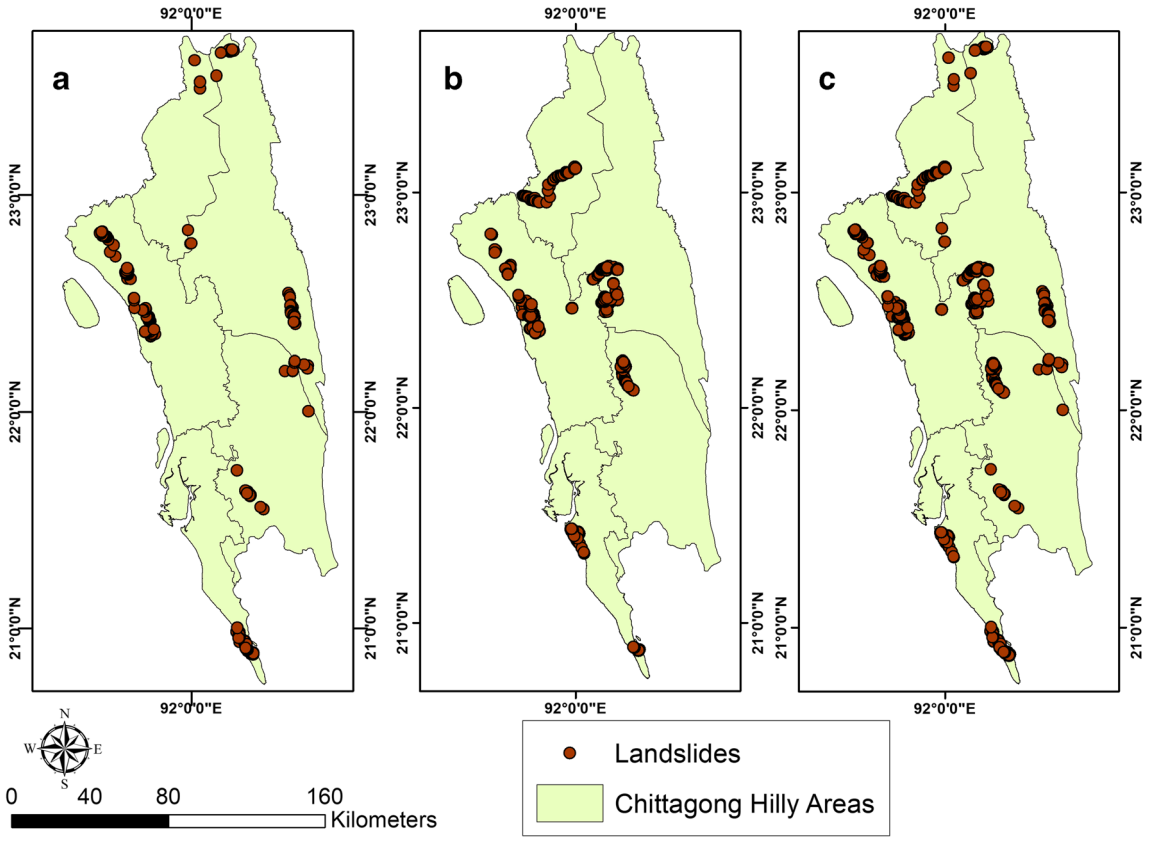

Fig. 6 Landslide inventory maps of Chittagong Hilly Areas of Bangladesh. (**a**) Landslide inventory map based on Google Earth. **b** Landslide inventory map based on field mapping. **c** Final landslide inventory map

the landslides we identified in the field were not mapped in Google Earth. These landslides were mainly close to the urban or rural settlements where the evidence of landslides is hard to be discriminated in Google Earth images.

In CMA, we mapped 63 landslides in Google Earth. We used 44 landslides field-mapped by Rahman et al. (2016) for validation. Among the 63 landslides, 9 landslides are at 0-m distance, and 30 landslides are < 100-m buffer distance from the field-mapped landslides (Table 3). The overall accuracy is 68.2% for the 100-m threshold buffer. The commission error is 52.4% and the omission error is 31.8% (Table 4). In Cox's Bazar municipality, we identified 54 landslides in Google Earth and used 64 landslides identified by field mapping of CDMP-II (2012) for validation. Among these 54 landslides, 7 are at 0-m distance, and 44 are < 100-m buffer distance from the landslide identified in the field mapping (Table 3). The overall accuracy is 68.7% for the 100-m threshold buffer. Here, commission error is 18.5% and omission error is 31.3% (Table 4).

Table 2 Distribution of landslides identified in Google Earth and field mapping among districts of Chittagong Hilly Areas

Districts	Google Earth	Field mapped
Chittagong	121	137
Bandarban	22	101
Cox's Bazar	48	77
Khagrachari	6	82
Rangamati	33	151

The higher accuracy in our test site than the two other areas is likely caused by the different field mapping methods at each site. We mapped landslides in Google Earth and validated all these landslides at the test site in Bandarban. The field-mapped landslides in CMA and Cox's Bazar municipality were likely only those causing casualties. In Cox's Bazar, the field map of CDMP-II (2012) included landslides in high-density urban areas, but we could not identify them in Google Earth. Although Google Earth has high-resolution images for urban areas, it may not be enough to detect landslides in high-density urban areas. Therefore, field mapping is still the best option to detect landslides in high-density urban areas. The omission errors range from 12 to 31% in these three sites, indicating that we may miss 10–30% of the landslides in Google Earth, especially in urban areas.

Discussion and conclusions

We produced a landslide inventory map of CHA in Bangladesh based on Google Earth imagery and field mapping. In our study, field mapping helped to identify more landslides than Google Earth mapping. In June 2017, numerous landslides occurred in

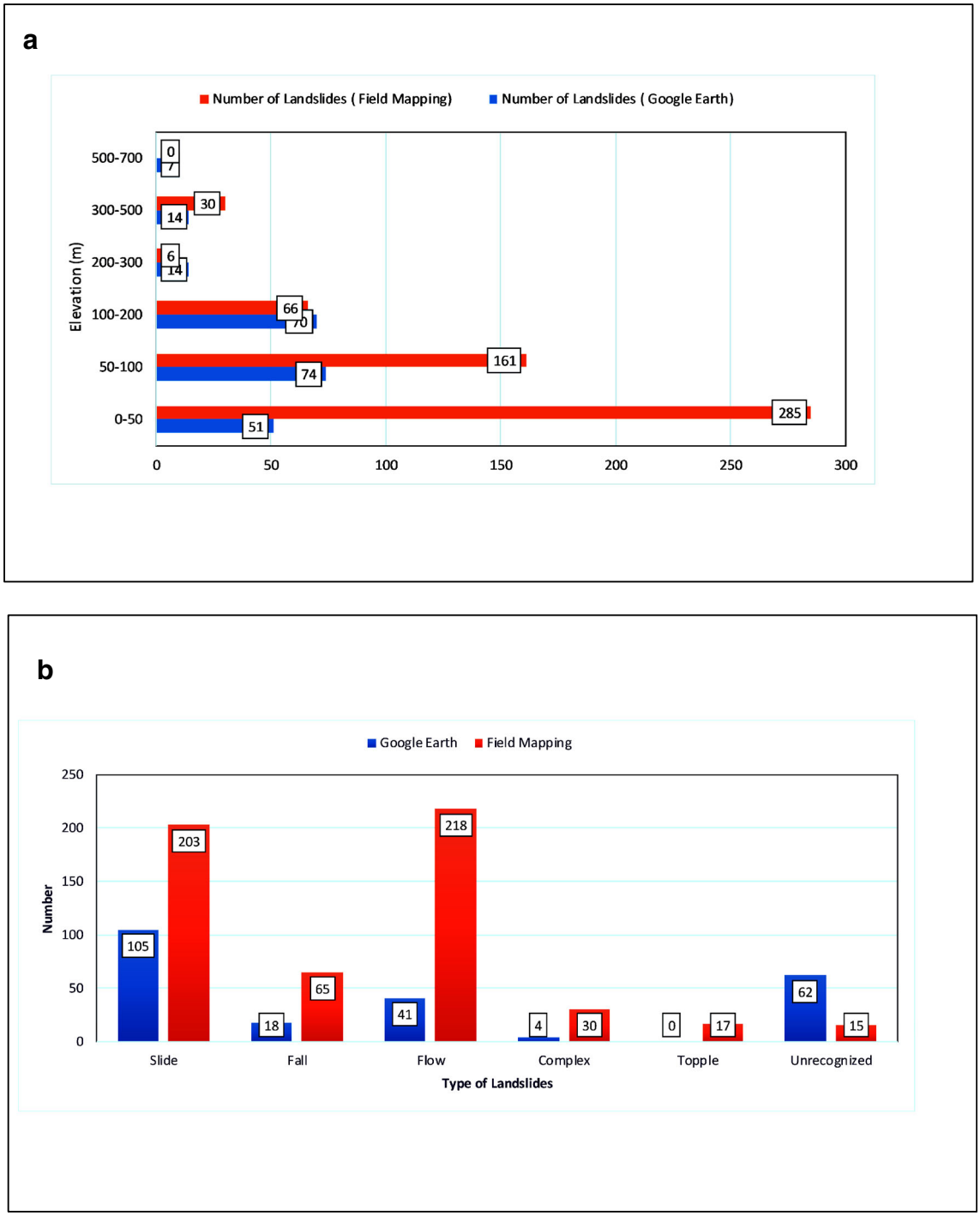

Fig. 7 Different statistics of identified landslides in Google Earth and field mapping. **a** Number of landslides at different elevation (Google Earth and field mapping) based on ASTER 30-m DEM. **b** Number of different types of landslides (Google Earth and field mapping)

five districts of the study area and we were able to identify these landslides in the field. In Bangladesh, vegetation regrows very quickly, and in urban areas, the rate of anthropogenic land-use change is extremely high, so any sign of a landslide may quickly disappear. As our field work was conducted just 1 month after the occurrence of the new landslides, we mapped more landslides in the field than in Google Earth. In addition, uncertainties and biases may exist in using Google Earth. Historical Google Earth imagery may not have continuity. Specifically, there is no regular monthly or yearly interval among two historical images, and the time gap between two historical images can be up to several years. Landslides that may occur within such a large time gap cannot be included in the inventory due to the fast vegetation regrowth, and the signs of the landslide may not be found in the next available

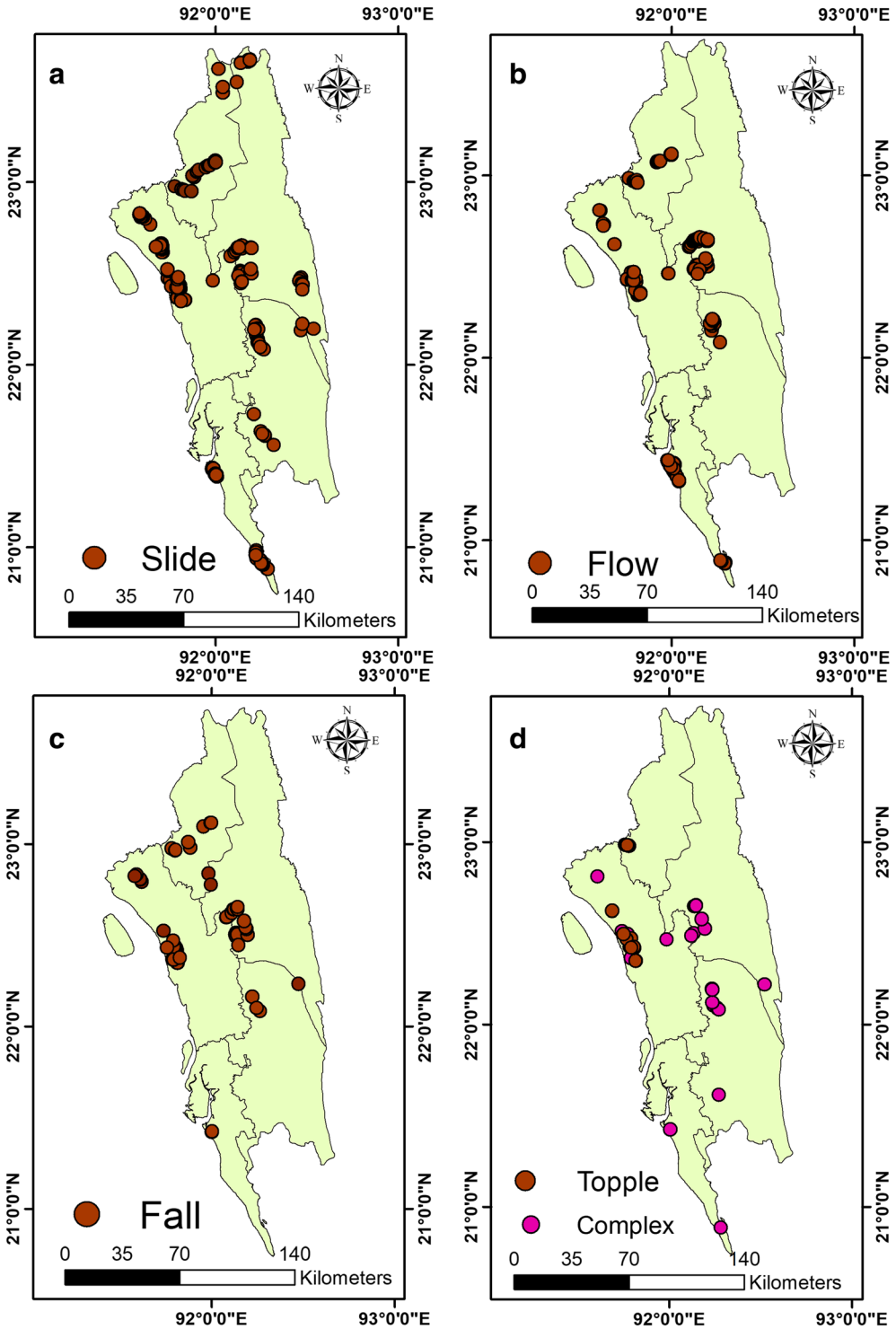

Fig. 8 Distribution of different types of landslides in Chittagong Hilly Areas of Bangladesh. **a** Slide. **b** Flow. **c** Fall. **d** Topple and Complex

image. Thus, the inventory generated just using Google Earth may not include all landslides.

Limitations still exist in our study. Google Earth-based mapping does not provide good results in urban areas where field mapping is more efficient. In contrast, field mapping is mainly conducted along roads and in urban and other accessible areas, whereas it is difficult in inaccessible areas in mountains covered by dense forest. Therefore, the integration of these two methods helps improve the landslide inventory mapping. However, although Google Earth can be used to map landslides in inaccessible areas, it is only applicable where landslides left clear and fresh footprints on the Google

Table 3 Percentage of landslide locations at different distance from ground points in Bandarban, CMA, and Cox's Bazar

Study site	Distance (m)	0	1–10	10–20	20–50	50–100	Above 100
Bandarban	Number of landslides	8	1	3	4	6	3
	Percentage	32.0	4.0	12.0	16.0	24.0	12.0
	Cumulative percentage	32.0	36.0	48.0	64.0	88.0	100.0
CMA	Number of landslides	9	5	3	5	8	14
	Percentage	20.5	11.6	6.8	11.4	18.2	31.9
	Cumulative percentage	20.5	31.8	38.6	50.0	68.2	100.0
Cox's Bazar	Number of landslides	7	18	8	8	3	20
	Percentage	10.9	28.1	12.5	12.5	4.7	31.3
	Cumulative percentage	10.9	39.0	51.5	64.0	68.7	100.0

Earth imagery. Time gaps between two images in Google Earth may exclude some landslides due to the fast vegetation recovery. The field mapping may not fill this gap because it mostly captured recent landslides. Another limitation comes from the uneven level of information collected by field mapping and Google Earth. In field mapping, we conducted in-depth assessment with local people and had a closed view to determine the cause and type of the landslides. In contrast, it is hard to determine the cause and type of the landslides simply by viewing the surrounding areas in Google Earth. Therefore, compared to only 2.7% of the landslides we mapped in the field, up to 26.0% of the landslides mapped in Google Earth do not include the type information.

We developed a set of criteria to identify landslides using Google Earth imagery. These criteria can be adopted to other areas, especially developing countries where high-resolution satellite imagery and aerial photographs are not available. We introduced a method to separate areas under the jhum cultivation from landslides. It can help landslide detection in areas where slash and burning are practiced. We also developed an accuracy assessment method based on a 100-m buffer distance threshold for landslides that are mapped as points rather than polygons in the field. Detail topographic maps are not available for some areas, especially developing countries, and the polygons cannot be drawn around the landslides in the field. Our assessment method would be helpful for this type of scenarios.

This work produced an updated landslide inventory of CHA. Previous studies mainly covered three urban areas and we expanded the mapping to all districts in CHA. We found that the Rangamati district has the second highest number of landslides, although relatively few studies were conducted there. We mapped 211 landslides in Bandarban and Khagrachari districts, which accounted for about 27% of the total landslides in CHA. This work helps refine the spatial distribution of landslides in our study area. Future work is needed to conduct the morphometric and engineering analysis on the landslides in these new areas.

Table 4 Accuracy assessment table for Bandarban, CMA, and Cox's Bazar (Column: Field mapping; Row: Google Earth)

Study sites		Landslide	Non-landslide	Total	Commission error (%)
Bandarban	Landslide	22	0	22	0.0
	Non-landslide	3	–		
	Total	25			
	Omission error (%)	12.0			
CMA	Landslide	30	33	63	52.39
	Non-landslide	14	–		
	Total	44			
	Omission error (%)	31.82			
Cox's Bazar	Landslide	44	10	54	19.52
	Non-Landslidl	20	–		
	Total	64			
	Producer's accuracy (%)	68.75			
	Omission error (%)	31.25			

Acknowledgements

The authors are grateful to Dr. Syed Humayun Akhter from the Department of Geology, University of Dhaka, and Mr. Azad Siddiq, Deputy Planner of the Rangamati Municipality, Bangladesh for their valuable suggestions and support during field work. We would like to thank the data collectors and field assistants; without their help this work would not have been possible. We also thank the editor and two anonymous reviewers for their constructive comments that significantly improve this paper.

Funding information

This work is funded by the W.K. McClure Scholarship program of the University of Tennessee, Knoxville.

References

Ahmed B (2015) Landslide susceptibility mapping using multi-criteria evaluation techniques in Chittagong Metropolitan Area, Bangladesh. Landslides 12:1077–1095. https://link.springer.com/content/pdf/10.1007%2Fs10346-014-0521-x.pdf. Accessed 27 Jan 2018

Ahmed B, Dewan A (2017) Application of bivariate and multivariate statistical techniques in landslide susceptibility modelling in Chittagong City Corporation, Bangladesh. Remote Sens. http://www.mdpi.com/2072-4292/9/4/304/htm. Accessed 29 Nov 2018

Alkevi T, Ercanoglu M (2011) Assessment of ASTER satellite images in landslide inventory mapping: Yenice Gokcebey (Western Black Sea region: Turkey). Bull Eng Geol 70:607–617. https://www.infona.pl/resource/bwmeta1.element.springer-7a652fd4-147e-35ca-8623-b3a758c2a0db. Accessed 29 Nov 2018

Bailey JE, Whitmeyer SJ, Paor DG (2012) Introduction: the application of Google Geo tools to geosciences education and research. In: Whitmeyer SJ, Bailey JE, Paor DG, Ornduff T (eds) Google earth and virtual visualizations in geosciences and education research. The geological survey of America. https://doi.org/10.1130/2012.2492(00)

Banglapedia (2015) Landslide, Banglapedia: National Encyclopaedia of Bangladesh. Asiatic Society of Bangladesh. http://en.banglapedia.org/index.php?title=Landslide. Accessed 10 March 2018

Brammer H (2012) The physical geography of Bangladesh. The University Press Limited, Dhaka

CDMP-II (2012) Comprehensive disaster management programme-II (CDMP-II). A report on the Landslide inventory and land-use mapping, DEM preparation, precipitation threshold value and establishment of early warning devices. Ministry of Food and Disaster Management, Disaster Management and Relief Division, Government of the People's Republic of Bangladesh

Carrara A, Cardinali M, Guzzetti F (1992) Uncertainty in assessing landslide hazard and risk. ITC Journal, The Netherlands 2:172–183. http://geomorphology.irpi.cnr.it/publications/repository/public/journals/1992/carrara_etal_uncertaintyaccessinglandslidehazardrisk_itc_1992.pdf. Accessed 29 Nov 2018

Crosby CJ (2012) Lidar and Google Earth: Simplifying access to high-resolution topography data. In: Whitmeyer SJ, Bailey JE, Paor DG, Ornduff T (eds) Google earth and virtual visualizations in geosciences and education research. The Geological survey of America, vol 492, pp 37–48. https://doi.org/10.11301/2012.2492(03)

Cruden DM, Varnes DJ (1996) Landslide types and processes. In: Turner AK, Schuster RL (eds) Landslides, investigation and mitigation, special report 247. Transportation Research Board, Washington D.C, pp 36–75 ISSN: 0360-859X, ISBN: 030906208X

Duric D, Mladenovic A, Pesic-Georgiadis M, Marjanovic M, Abolmasov B (2017) Using multi-resolution and multi-temporal satellite data for post-disaster landslide inventory in the republic of Serbia. Landslides 14:1467–1482. https://link.springer.com/content/pdf/10.1007%2Fs10346-017-0847-2.pdf. Accessed 29 Nov 2018

Environmental System Reserach Institute (ESRI) (2014) ArcGIS Desktop Help 10.2 Geostatistical Analyst.https://resources.arcgis.com/en/help/main/10.2/index.html#//00080000001q000000. Accessed 28 Nov 2018

Fisher GB, Amos CB, Bookhagen B, Burbank DW, Godrad V (2012) Channel widths, landslides, faults, and beyond: The new world order of high spatial resolution Google Earth imagery in the study of earth surface process. In: Whitmeyer SJ, Bailey JE, Paor DG, Ornduff T (eds) Google earth and virtual visualizations in geosciences and education research. The geological survey of America, vol 492, pp 1–22. https://doi.org/10.11301/2012.2492(01)

Fox J, Truong DM, Rambo AT, Tuyen NP, Cuc LT, Leisz S (2000) Shifting cultivation: a new old paradigm for managing tropical forest. Bioscience 50(6):521–528. https://doi.org/10.1641/0006-3568(2000)050[0521:SCANOP]2.0.CO;2. Accessed 14 Sept 2017

Galli M, Ardizzone F, Cardinali M, Guzzettie F, Reichenbach P (2008) Comparing landslide inventory maps. Geomorphology 94(2008):268–289 https://ac.els-cdn.com/S0169555X07002681/1-s2.0-S0169555X07002681-main.pdf?_tid=fd39dfd0-0565-11e8-87d3-00000aacb360&acdnat=1517279803_3b62cd. Accessed 12 May 2017

Glade T (1998) Establishing the frequency and magnitude of landslide-triggering rainstorm events in New Zealand. Environ Geol 35(2–3):160–174. https://link.springer.com/content/pdf/10.1007/s002540050302.pdf. Accessed 20 Feb 2018

Guzzetti F, Mondini AC, Cardinali M, Fiourucci F, Santangelo M, Chang KT (2012) Landslide inventory maps: new tools for an old problem. Earth Sci Rev 112(2012):42–66 https://ac.els-cdn.com/S0012825212000128/1-s2.0-S0012825212000128-main.pdf?_tid=8007b706-0567-11e8-a3a7-00000aab0f02&acdnat=1517280452_cfd52e934353fa5382085ac85f69aa18. Accessed 3 April 2017

Kanwal S, Atif S, Shafiq M (2016) GIS based landslide susceptibility mapping of northern areas of Pakistan, a case study of Shigar and Shyok basins. Geomat Nat Haz Risk 8:348–366. https://doi.org/10.1080/19475705.2016.1220023. Accessed 29 Nov 2018

Khan YA, Lateh H, Baten MA, Kamil AA (2012) Critical antecedent rainfall conditions for shallow landslides in Chittagong City of Bangladesh. Environ Earth Sci 67:97–106. https://www.researchgate.net/publication/257793592_Critical_antecedent_rainfall_conditions_for_shallow_landslides_in_Chittagong_City_of_Bangladesh. Accessed 29 Nov 2018

Masum KM, Rashid MM, Jashimuddin M, Ara SJG (2011) Land use conflicts of Chittagong Hill tracts and indigenous hill people as victim in Bangladesh. J Gen Educ 1:62–71 https://www.researchgate.net/publication/235703063_Land_use_conflicts_of_Chittagong_Hill_Tracts_and_indigenous_hill_people_as_victim_in_Bangladesh. Accessed 29 Nov 2018

Rahman MS, Ahmed B, Huq FF, Rahman S, Al-Hussain TM (2016) Landslide inventory in an urban setting in the context of Chittagong Metropolitan, Area, Bangladesh. In the proceedings of 3rdInternational conference in Civil Engineering, 21–23 December 2016 CUET, Chittagong, Bangladesh. https://www.researchgate.net/publication/308171472_Landslide_Inventory_in_an_Urban_Setting_in_the_Context_of_Chittagong_Metropolitan_Area_Bangladesh. Accessed 27 March 2017

Samodra G, Chen G, Sartohadi J, Kasama K (2015) Generating landslide inventory by participatory mapping: an example in Purwosari Area, Yogyakarta, Java. Geomorphology 306:306–313. https://doi.org/10.1016/j.geomorph.2015.07.035. Accessed 10 Jan 2018

Sato HP, Harp EL (2009) Interpretation of earthquake-induced landslides triggered by the 12 May 2008, 7.9 Wenchuan earthquake in Beichuan area, Sichuan Province, China using satellite imagery and Google Earth. Landslides 6:153–159. https://link.springer.com/article/10.1007/s10346-009-0147-6. Accessed 2 Feb 2018

Vakhshoori V, Zare M (2016) Landslide susceptibility mapping by comparing weight of evidence, fuzzy logic, and frequency ratio methods. Geomat Nat Haz Risk 7(5):1731–1752. https://doi.org/10.1080/19475705.2016.1144655. Accessed 7 Aug 2018

Wang Y, Zou Y, Henrickson K, Wang Y, Tang J, Park BJ (2017) Google earth elevation data extraction and accuracy assessment for transportation application. PLoS One 12(14):e0175757. https://doi.org/10.1371/journal.pone.0175756. Accessed 29 Nov 2018

Y. W. Rabby (✉) · **Y. Li**
Department of Geography,
University of Tennessee,
Knoxville, TN, USA
Email: yrabby@vols.utk.edu

Y. Li
e-mail: yli32@utk.edu